Institute of Engineering Geodesy (IIGS)

1. Members of Staff

Head of Institute:	Prof. Dr.-Ing. habil. Volker Schwieger

Secretary:	Elke Rawe
	Ute Schinzel
Emeritus:	Prof. Dr.-Ing. Dr.sc.techn.h.c. Dr.h.c. Klaus Linkwitz

Scientific Staff:	M.Sc. Ashraf Abdallah	GNSS Positioning
	M.Sc. Bara' Al-Mistarehi	Construction Process
	M.Sc. Aiham Hassan	Monitoring
	Dipl.-Ing. Stephanie Kauker	Monitoring
	Dipl.-Ing. Otto Lerke	Machine Guidance
	M.Sc. Xiaojing Lin (until 28.02.2015)	Machine Guidance
	Dr.-Ing. Martin Metzner	Engineering Geodesy
	Dipl.-Ing. Annette Scheider	Kinematic Positioning
	M.Sc. Pham Trung Dung	Kinematic Positioning
	M.Sc. Annette Schmitt	Multi-Sensor-Systems
	M.Sc. Rainer Schützle	Location Referencing
	M.Sc. Jinyue Wang (since 01.06.2015)	Map Matching
	Dipl.-Ing. Li Zhang	Monitoring
	Dipl.-Ing. Bimin Zheng (until 31.03.2015)	Monitoring

Technical Staff:	Andreas Kanzler
	Martin Knihs
	Lars Plate

External Teaching Staff:	Dipl.-Ing. Jürgen Eisenmann	Landratsamt Ostalbkreis,– Geoinformation und Landentwicklung
	Dipl.-Ing. Christian Helfert	Fachdienstleiter Flurneuordnung im Landkreis Biberach
	Dipl.-Math. Ulrich Völter	Geschäftsführer der Fa. Intermetric
	Dr.-Ing. Thomas Wiltschko	Daimler AG, Mercedes-Benz Cars; Research and Development

2. General View

The Institute of Engineering Geodesy (IIGS) is directed by Prof. Dr.-Ing. habil. Volker Schwieger. It is part of the Faculty 6 "Aerospace Engineering and Geodesy" within the University of Stuttgart. Prof. Schwieger holds the chair in "Engineering Geodesy and Geodetic Measurements". In 2012 he was elected Vice Dean of Faculty 6.

In addition to being a member of Faculty 6, Prof. Schwieger is co-opted to Faculty 2 "Civil and Environmental Engineering". Furthermore, IIGS is involved in the Center for Transportation Research of the University of Stuttgart (FOVUS). Prof. Schwieger presently acts as speaker of FOVUS. So, IIGS actively continues the close collaboration with all institutes in the field of transportation, especially with those belonging to Faculty 2.

Since 2011 he is full member of the German Geodetic Commission (Deutsche Geodätische Kommission – DGK). Furthermore, Prof. Schwieger is a member of the section „Engineering Geodesy" within the DGK. He is head of the DVW working group 3 "Measurement Techniques and Systems" and chairman of the FIG Commission 5 "Positioning and Measurements" for the period 2015-2018.

The institute's main tasks in education focus on geodetic and industrial measurement techniques, kinematic positioning and multi-sensor systems, statistics and error theory, engineering geodesy and monitoring, GIS-based data acquisition, and transport telematics. Here, the institute is responsible for the above-mentioned fields within the curricula of "Geodesy and Geoinformatics" (Master and Bachelor courses of study) as well as for "GEOENGINE" (Master for Geomatics Engineering in English). In addition, the IIGS provides several courses in German for the curricula of "Aerospace Engineering" (Bachelor and Master), "Civil Engineering" (Bachelor and Master), "Transport Engineering" (Bachelor and Master) and "Technique and Economy of Real Estate" (Bachelor). Furthermore, lectures are given in English to students within the master course "Infrastructure Planning". Finally, eLearning modules are applied in different curricula.

The current research and project work of the institute is expressed in the course contents, thus always presenting the actual state-of-the-art to the students. As a benefit of this, student research projects and theses are often implemented in close cooperation with the industry and external research partners. The main research focuses on kinematic and static positioning, analysis of engineering surveying processes and construction processes, machine guidance, monitoring, transport and aviation telematics, process and quality modeling. The daily work is characterized by intensive co-operation with other engineering disciplines, especially with traffic engineering, civil engineering, architecture and aerospace engineering.

3. Research and Development

3.1. Improving the Quality of Low-Cost GPS Receiver Data Using Spatial Correlations

The investigations on low-cost single frequency GPS receivers at the Institute of Engineering Geodesy (IIGS) show that u-blox LEA-6T GPS receivers combined with Trimble Bullet III GPS antennas containing self-constructed L1-optimized choke rings can already obtain an accuracy in the range of millimeters which meets the requirements of geodetic precise monitoring applications. However, the quality (accuracy and reliability) of low-cost GPS receiver data, particularly in shadowing environment, should still be improved, since the multipath effects are the major error for the short baselines.
For this purpose, as shown in Figure 1, a 3 × 3 antenna array was set up next to the metal wall on the roof of the IIGS building, with a distance between two antennas of 0.5 m, so the antenna array has an extension of 1 m × 1 m. Static measurement was carried out for 26 days (from 3 March to 1 April 2014). The GPS raw data were recorded from the 9 receivers at 1 Hz, stored on a PC, evaluated and post-processed. One SAPOS station is only about 500 m away from the test field. This station is taken as reference station and the 9 stations in

the test field are taken as rover stations for processing the baselines, so that 9 baselines can be obtained.
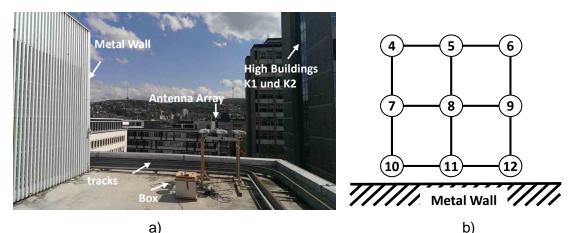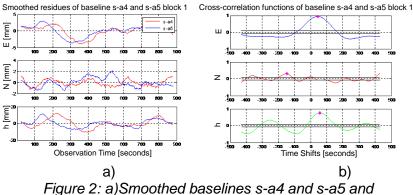

a)   b)

Figure 1: Photos of test field with antenna array a) and Antenna number b).

The time series of three-dimensional coordinates of the GPS receivers were analysed. The coordinate residuals contain both non-correlating and correlating errors. Only the correlated errors are of interest. The non-correlating errors are reduced by using the moving average filter. By analysing the coordinates, it is noticed that the coordinates often contain oscillations with periods of 30 to 40 seconds. These periods are probably caused by the multipath effects from the two high buildings. These periods are so short that they are not really of interest for monitoring. For this reason, 40 seconds are chosen as window size of the moving average. In Figure 2 the smoothed baselines s-a4 and s-a5 and their cross-correlation functions of the first 15-minutes block are shown.

It can be found out that their residuals can be quite similar (compare east and height component) but sometimes are not (compare north component), and there are time shifts between their errors. That means that similar errors can be present in baseline s-a4 as well as in baseline s-a5 with a time shift.

a)   b)

Figure 2: a)Smoothed baselines s-a4 and s-a5 and
b) Cross-correlation functions between them

Block 1 is just an example, the time shifts vary from block to block and can be positive or negative as well as zero. The correlations of each coordinate component also vary from block to block. They depend on the geometry of satellite-antenna-reflectors.

Thus, the idea of the algorithm is that the coordinates of one station (station A) can be corrected using the spatial correlations of coordinates of an adjoined station (station B), so that the accuracy and reliability of the GPS measurement is improved:

$$kr_{\overline{SA},j,q}(t) = k_{\overline{SA},j,q}(t) - m_{j,q} \cdot k_{\overline{SB},j,q}(t + \Delta t). \tag{1}$$

As shown in Equation (1), $k_{\overline{SA},j,q}(t)$ and $k_{\overline{SB},j,q}(t)$ are residuals of two baselines in j-component (j=E,N,h) and q block (q=1,2, …96). These residuals are free from the mean val-

ue. The geometric relationship between the stations S, A, B is used to correct part of the errors from the GPS processing. This will not be explained here. It can be derived from the cross-correlation function that the two residuals $k_{\overline{SA},j,q}(t)$ and $k_{\overline{SB},j,q}(t)$ have the maximum correlation at time shift Δt. $k_{\overline{SB},j,q}(t)$ will be taken and shifted about Δt, so that we can achieve $k_{\overline{SB},j,q}(t + \Delta t)$. It is assumed that there is scale $m_{j,q}$ between $k_{\overline{SA},j,q}(t)$ and $k_{\overline{SB},j,q}(t + \Delta t)$, so $k_{\overline{SB},j,q}(t + \Delta t)$ will be scaled and used to correct the $k_{\overline{SA},j,q}(t)$, therefore the corrected residuals for the baseline SA is $kr_{\overline{SA},j,q}(t)$. The maximum of the cross-correlation function can be taken as scale $m_{j,q}$, or $m_{j,q}$ can be estimated by adjustment. The scale calculated by adjustment provides better results, since the scale larger than 1 (compare Equation (1)) is a possible solution for some cases. This cannot be delivered by correlation functions.

For example, a4 and a5 are regarded as station A and B. The residuals of baseline s-a5 can be taken to correct the residuals of baseline s-a4. In Figure 3a) the residuals of baseline s-a5 are shifted by Δt and compared with the baseline s-a4. The residuals of baseline s-a4 $k_{\overline{sa4},j,q}(t)$ and the corrected s-a4 $kr_{\overline{sa4},j,q}(t)$ using $k_{\overline{sa5},j,q}(t)$ according to Equation (1) are shown in Figure 3b). The performance of this algorithm is dependent on the spatial correlation. In Figure 3b) it can be seen that oscillations in the east and height component are significantly suppressed, since the correlations between these two components are very high. The correction does not work well in the north component, since the correlation is quite low.
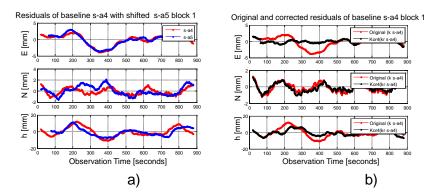

Figure 3: a) Residuals of baseline s-a4 with shifted s-a5 and
b) original and the corrected baseline s-a4

The spatial correlation varies from time to time. Thus, the performance of the algorithm is evaluated for all 96 blocks. The standard deviations of baseline s-a4 can be improved on average by about 50% by using the spatial correlation with baseline s-a5.

3.2. Effect of Satellite Clocks on Kinematic PPP solution for the Hydrographic Survey

Since the GNSS technique provides the position of objects with high accuracy, this technique has become one of the most important techniques to obtain hydrographic information. Over the last two decades, the precise point positioning (PPP) technique, which uses only a single receiver has gained an increase of interest. To obtain the centimeter accuracy level, a dual frequency GNSS instrument is required. The sampling rate of the satellite clocks affects the accuracy of kinematic PPP solution. The precise satellite orbits and clocks may be provided from the International GNSS Service (IGS). A comparison between the Bernese GNSS V. 5.2 software and CSRS-PPP online service has been carried through. During the processing, the satellite clocks provided by IGS with a sampling rate of 30 seconds were used.

In order to identify the accuracy of kinematic PPP solution for hydrographic survey, three kinematic trajectories were observed on the Rhine River, Duisburg, Germany as a part of project "HydrOs - Integrated Hydrographical Positioning System". This project is launched in co-operation between the department M5 (Geodesy) of the German Federal Institute of Hydrology (BfG) and the Institute of Engineering Geodesy at the University of Stuttgart (IIGS).

An antenna of LEIAX1203+GNSS and a receiver LEICA GX1230+GNSS were located on the surveying vessel (Mercator) to collect the GNSS data. Figure 4 presents the surveying vessel and the GNSS antenna over it.

Figure 4: "Mercator" observation vessel for the measurement data (left figure); GPS antenna over the vessel (right figure)

Table 1 presents the statistical results, Root mean square (RMS) as well as standard deviation σ, obtained from Bernese GNSS software and CSRS-PPP online service. These results are calculated relative to the double-difference solution from Bernese software.

		TRAJ1			TRAJ2			TRAJ3		
		East	**North**	**height**	**East**	**North**	**height**	**East**	**North**	**height**
Bernese GNSS	**RMS [m]**	0.081	0.104	0.010	0.10	0.09	0.113	0.050	0.052	0.149
	σ **[m]**	0.081	0.096	0.096	0.068	0.075	0.107	0.050	0.052	0.144
CSRS-PPP	**RMS [m]**	0.182	0.114	0.068	0.082	0.082	0.087	0.023	0.026	0.041
	σ **[m]**	0.098	0.104	0.063	0.066	0.072	0.087	0.022	0.022	0.033

Table 1: Statistical results from Bernese GNSS software and CSRS-PPP online service.

As shown in Figure 5, Bernese solution delivers in average a standard deviation of 7 cm for the horizontal components, and 12 cm for vertical components. CSRS-PPP online service provides a better solution than that obtained by Bernese software. It shows in average a standard deviation of 6 cm in all components.
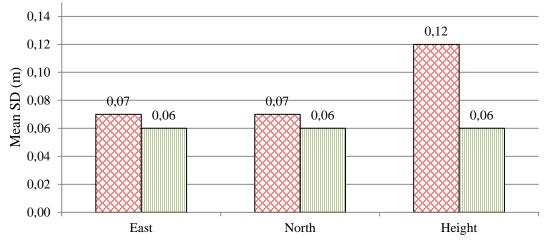
Figure 5: Mean SD for Bernese GNSS and CSRS-PPP online service.

3.3. Integration of additional sensors in the HydrOs system

The system HydrOs includes a multi-sensor system and an evaluation software to determine continuously the position and the spatial orientation of a surveying vessel on inland waterways. This system is able to bridge gaps in GNSS-RTK measurements so that reliable coordinates are also available in GNSS shadowed areas or in areas without reception of a GNSS reference service (e. g. SA*POS*®). This system has been developed by IIGS and the Federal Institute of Hydrology (BfG).

Now new optional components are integrated into the system and analysed. Next to additional filtering algorithms (software components) also new sensors are tested: A camera is mounted on the vessel and takes images of the riverside in short time intervals. These images are evaluated with Agisoft PhotoScan to estimate the exterior orientation of each image. If known points along the riverside or some known camera positions are used to georeference the data, the complete trajectory of camera positions will be determined in the UTM coordinate system. This information is integrated as additional position observation into the HydrOs software. Thus, coordinates should be available also in parts of the trajectory which do not contain any valid GNSS positions..

Because only reliable coordinates can be used, the resulting camera coordinates must be determined carefully: Poor environmental conditions may cause unreliable camera coordinates. According to the time of capturing and the shape of the river, the light conditions change suddenly and can be challenging (shadowed areas, sun shines directly into the objective lens). Low image overlaps may also be a problem. Besides, the timing component must be considered: To improve the results of the Extended Kalman Filter (EKF) in the HydrOs software, each camera position must have a precise time stamp.
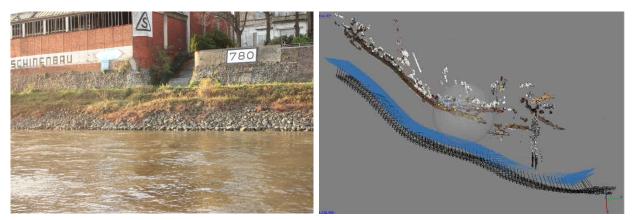
Figure 6: Photo of the riverside in Duisburg-Homberg

Figure 7: Trajectory of camera positions, evaluated with Agisoft PhotoScan

To test the performance of the system, measurement data was captured on the river Rhine close to Duisburg-Homberg (Figure 6). In this area, the vessel was driving approximately in north-south direction.

By integrating these data (Figure 7) into the HydrOs software, the estimated coordinates can be improved. For this reason, the EKF results are compared to the results of the default HydrOs sensor configuration without camera. After a simulated gap of approx. 1 minute in the GNSS measurement data, the maximal deviation in the transversal direction (Easting) of the trajectory is decreased to 55.7 % and 34.5 % respectively.

3.4. Construction of a Synthetic Covariance Matrix for Terrestrial Laserscanning

This work is part of the project IMKAD, which is funded by the Deutsche Forschungsmeinschaft (DFG) and realized in cooperation of the Institute of Engineering Geodesy, University of Stuttgart, with the Department of Geodesy and Geoinformation, Vienna University of Technology.

Considering the correlations within a terrestrial laserscanning point cloud requires a synthetic covariance matrix. This matrix contains variances and co-variances computed from the main influences on terrestrial laserscanning measurements. Building a synthetic covariance matrix is based on the elementary error model. In order to construct a synthetic covariance matrix, all considered error sources should be classified into different groups regarding their type of correlation. A distinction is made between non-correlating, functional correlating and stochastical correlating groups, in which each group is expressed by one variance/co-variance matrix.

Applying the elementary error model on terrestrial laserscanning measurements requires the determination of the main impacts. For this reason, it is assumed that the functionality of a terrestrial laser scanner is mainly similar to the one of a tachymeter. Hereby, most of the instrumental impacts, such as range error, collimation axis error and vertical index error are classified to the functional group. Range noise and angular noise, on the other hand, define non-correlating errors. Moreover, the atmospheric impacts and object-based impacts are classified to the stochastic correlating group. Nevertheless, the atmospheric impacts are modeled functionally at the time of writing due to homogeneous laboratory measurement conditions. Furthermore, object-based impacts like color, penetration depth, reflectivity and roughness are combined to one influencing parameter since it has not been possible to separate them yet. Another essential impact is caused by the angle of incidence between the laser beam hitting the object's surface and its normal vector of the same point. Next, the functional relations between the elementary errors and the observations are necessary, in order to calculate numerical influences, variances and co-variances respectively. Summing up all variance/co-variance matrices results in the synthetic covariance matrix Σ_{ll}, as shown below in Equation (2):

$$\Sigma_{ll} = \sum_{k=1}^{p} D_k \cdot \Sigma_{\delta\delta,k} \cdot D_k^T + F \cdot \Sigma_{\xi\xi} \cdot F^T + \sum_{h=1}^{q} G_h \cdot \Sigma_{\gamma\gamma,h} \cdot G_h^T \ . \tag{2}$$

By means of this, an error of position regarding each point within the point cloud can be calculated. Furthermore, the correlation matrix can be determined by standardization of the synthetic covariance matrix (see Equation (3)).

$$R_{ll} = \frac{1}{\sqrt{diag(\Sigma_{ll})}} * \Sigma_{ll} * \frac{1}{\sqrt{diag(\Sigma_{ll})}} \tag{3}$$

Its structure, which is equal to the one of Σ_{ll}, provides the computation of correlations of each coordinate axis. Figure 8 shows first results of a modelled rectangle with the size of 30 cm x 25 cm regarding spatial correlations of the collimation axis. Due to the spot size of about 9 mm of the laser beam at a distance of 10 m the chosen point distance of 12 mm for modelling is justified. As result, the error of position reaches 4 mm over the entire area. In addition, the small size of the grid causes high spatial correlations regarding the collimation axis.
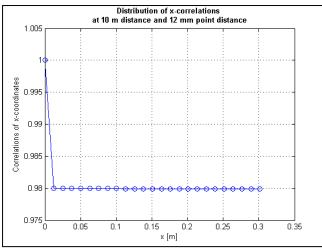

Figure 8: Correlations of x-coordinates depending on their distances to each other

In future work, temporal correlations as well as optimizing the atmospheric model might be considered. Moreover, evaluating the synthetic covariance matrix by multiple scans is necessary in order to provide temporal correlations between observations. Furthermore, modelling real atmospheric impacts must be implemented by considering test bodies such as barrages and dams.

3.5. Comparison of Extended Kalman Filter, Unscented Kalman Filter and Particle Filter focusing on simulation of vehicle positioning

A comparison of three estimation algorithms including Extended Kalman filter (EKF), Unscented Kalman filter (UKF) and Particle filter (PF) is performed in term of accuracy and computational time (Table 3). The root mean square error (RMSE) is determined from estimated value and true value for all trajectory points as:

$$RMSE = \sqrt{\frac{\sum_{i=1}^{N}\left(\left(X_{true,i} - X_{est,i}\right)^2 + \left(Y_{true,i} - Y_{est,i}\right)^2\right)}{N}} \tag{4}$$

where X_{true}, Y_{true}: positions of the true trajectory
X_{est}, Y_{est}: estimated positions of EKF, UKF, and PF
N: the number of epochs.

PF		UKF	EKF
Number of Particles	Second		
100	2	2×10^{-2} second	3×10^{-3} second
200	4		
500	9		
1,000	18		

Table 3: Execution time of filtering algorithms using Matlab R2014 running on a standard PC with a 2.66GHz Intel Dual Core processor and 4GB RAM.

The linear model is defined by a linear predicted model and a linear measurement model. The linear predicted model is based on straight line function by varying the positions and the velocity. The linear measurement model is a function of observed positions.

A non-linear model consists of a circle line function for predicted models by varying the positions, the angle, the velocity and the different direction and the non-linear measurement model established by distance and horizontal angle of measurements.
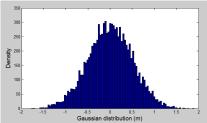

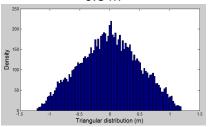*Figure 9: Histogram of Gaussian noise with the standard deviations of 0.5 m*

Figure 10: Histogram of non-Gaussian noise using triangle distribution with the standard deviations of 0.5 m
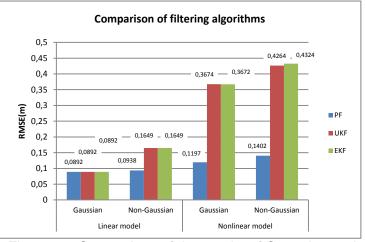

Figure 11: Comparison of the results of Gaussian and non-Gaussian distribution for the linear and non-linear models using the same standard deviations of 0.5 m.

From the simulation results, the performance of the accuracy and the computational time can be summarized as

- Performance of the accuracy:

  For the linear estimation, the estimated results of three filtering algorithms are comparable with Gaussian noise. In case of non-Gaussian noise, the best solution in term of accuracy belongs to PF. Two remaining algorithms are approximately equivalent.
  For the nonlinear estimation, the PF algorithm is the best solution with both Gaussian noise and non-Gaussian noise, especially to larger measurement standard deviation. UKF and EKF bring results with equivalent accuracy.

- Performance of the computational time:

EKF is the fastest method and followed by UKF. The burden of computational time is due to the large required number of particles, which becomes the main drawback of PF.

For the linear model with Gaussian and non-Gaussian, EKF and UKF are suitable methods both in terms of accuracy and computational time. In contrast, PF is an effective method in terms of accuracy according to the nonlinear model.

3.6. Construction Machine Simulator – Control of a Model Dozer

The IIGS construction machine simulator was developed to test and evaluate different sensors, filter and control algorithms. In the recent configuration the simulator comprises a model dozer, in the scale of 1:14, a Leica TCRP 1201 tachymeter as positioning sensor, a control computer and an A/D converter (Figure 12).
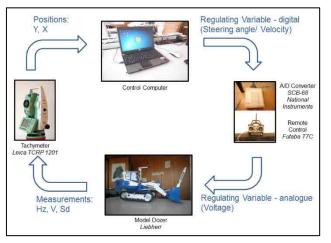

Figure 12: Hardware Components of the Recent Simulator Configuration

(Picture: Own Pictures)

The following new features have been implemented:
  (a) New suitable set of PID controller parameters for the lateral control algorithm
  (b) Longtidual control/speed control algorithm with an optionally selectable driving program
  (c) Tool control

The descriptions are split up into two thematic parts: the drive control including the features (a) and (b) and the tool control (feature (c)).

Drive Control

In previous works, a lateral control of a crawler model was implemented, allowing the vehicle to move automatically on a predefined trajectory. This is realized by different controllers, namely 2-point-, 3-point-, PID and Fuzzy. Due to the fact that a new crawler vehicle, „Liebherr 634", has been integrated into the simulator, new appropriate parameters for the PID controller had to be found. Figure 13 shows the impact of different PID parameter settings on the driving behaviour of the crawler. The following new PID parameters for the lateral control could be derived from test drive analyses:

Proportional gain: $K_P = 100,$
Integral gain: $K_I = 25$,
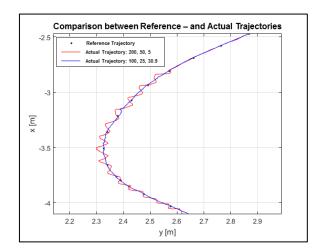Differential gain: $K_D = 30.9$.

Figure 13: Impact of PID Controller Parameter Settings on the Driving Behaviour

Additionally, a speed control algorithm, as well based on a PID controller, was integrated into the control program. Two functions have been included. The first function allows the user to choose a desired moving velocity. Consequently the vehicle moves constantly with the set speed along the reference trajectory. It has the ability to keep constant speed even in critical parts of the trajectory, e.g. curves. This function is extended by an optionally selectable driving program. The driving program is geometry based and allows the user to set speed and the desired number of laps. After passing the set number of laps it stops automatically at a defined end position. Thereby the acceleration and deceleration sequences are performed gradually, allowing smooth starts and stops.

For future works new transfer functions should be found to improve lateral and longitudinal guidance behaviour. For this, several calibration campaigns are planned.

Tool Control

The combination of a crawler chassis and the specific tool allows performing levelling works or loading processes. The focus of the recent report is on the levelling works.

The aim of levelling work is to produce a predefined plane or level for potentially following construction processes. This might be an area with equally distributed heights or a route or part of a route with differently distributed heights, e.g. slopes or ramps. Therefore the machine has to keep the working tool, more precise the bucket, in a predefined height and tilt position.

The investigated tool consists of a cantilever arm and a bucket, assembled on the tip of the cantilever arm. The cantilever arm is mounted to the frame by two swivel joints. These joints act concurrently as arm's pivots (Figure 14). By performing rotational movements around the pivots the arm can be lifted and lowered. The bucket is attached to the arm by two further swivel joints. This configuration allows rotational movements (tilts) of the bucket around these joints. Each of the components is driven by a separate hydraulic circuit. Both hydraulic circuits are supplied by a single hydraulic pump.
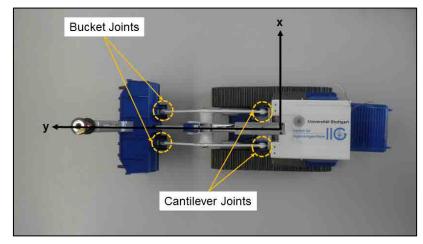
Figure 14: Position of the Swivel Joints (Top View) (Picture: Own Pictures)

Two sensors are fused to achieve control of the tool. For the control of the cantilever arm a tachymeter-reflector combination is used on the sensor side. The arm is controlled within a closed-loop system by the use of a PID controller. The bucket's control is realized by the attachment and alignment of an inertial measurement unit (IMU) alongside of the bucket. Therefore a second closed-loop-system is implemented. The control and regulation is realized by a 3-point controller. In this context, an important decision had to be made regarding the selection of the appropriate closed-loop controlled variable $y(t)$. It could be stated that incremental measurement techniques are not suitable for this specific kind of problem because any kind of movement, coming from the chassis or the cantilever arm, is detected and integrated by the incremental sensor. Hence, the ability to state whether the movement is performed by the bucket, by the vehicles or by its components, is not given. Based on these facts the decision fell on an absolute measurement value. The „Microstrain 3DM-GX2" IMU is able to indicate the Euler angles. These 3 angles are defined as „Roll", „Pitch" and „Yaw". Regarding the tilt movement of the bucket the decision was made to use the „Pitch" information as controlled variable $y(t)$.

In the next steps the tachymeter-reflector combination is to be replaced by an alternative measurement technique, e.g. sonic sensor, to avoid negative effects of the prism position on the drive control. Furthermore an appropriate transfer function is to be found to describe the cantilever movement mathematically.

3.7. An Approach for Automated Detection and Classification of Pavement Crack

Considerable developments and improvements have been made in the field of automated crack detection in the last years. Digital image processing techniques for crack detection are already widely adapted on large highways maintenance projects. Complete automated crack detection is only realized for continuous pavement images series by commercial companies. No standard scenario of digital image processing algorithms for crack detection is available and guarantees in all crack pavement images cases. Previously several image processing algorithms for crack detection are suffering from various shortcomings on crack detection sides. This work provides proposed automated image processing crack detection algorithm. The goal is to automatically extract and classify the linear crack and its characteristics from sequence pavement images of different streets. The sequence pavement images (mobile mapping data) were observed by two Germany companies as follows : LEHMANN + PART-NER GmbH company using S.T.I.E.R mobile mapper system and 3D Mapping Solutions GmbH company using MoSES mobile road mapping system. In addition, two case studies were observed by Unicom-Umap company using VISAT™ mobile mapping system -Saudi Arabia.

The overall proposed algorithm is used for testing various pavement crack images from different countries. The performance is checked by comparing the results with well-known crack detection algorithms. Obviously, the validation process is deviated by 3.8 min (processing time) and 98.9% (percentage of correctness rate) for around 96 continuous mobile mapping images (Lehmann + Partner GmbH company images-Germany). 16.2 min in average and 100% for around 336 continuous mobile mapping images (3D-mapping Solution GmbH company images-Germany) could be achieved. Moreover, in average 15.6 min and 100% for around 200 continuous mobile mapping images (Unicom-Umap company images-Saudi Arabia) could be obtained. Figure 15 illustrates the final resultant images with network of cracks (block type) and vertical individual cracks and their characterstics.

Figure 15: Final resultant images with vertical individual cracks and network of cracks (block type) and their characteristics.

3.8. Geodetic Control of FEM-Model from plane load-bearing structures

The goal of this investigation is to verify the simulation model with the reality. The investigated plane load-bearing structure is the thin double curved structure Stuttgart SmartShell. Stuttgart SmartShell has a base area of about 100 m² and a thickness of 4 cm. It is made of multilayer wood. Stuttgart SmartShell is resting on four supports. One of these supports is static, while the other three are mobile. The main reason to develop a structure like Stuttgart SmartShell is to investigate possibilities for constructions which offer an active manipulation in order to reduce structural vibrations and stress. In the same time the weight of the structure is drastically reduced. Figure 16 shows Stuttgart SmartShell.

Figure 16: Stuttgart SmartShell (© Bosch Rexroth).

The mobile supports of Stuttgart SmartShell can be moved in the three directions X, Y and Z. During the investigation with the Laser Scanner Leica HDS 7000, all supports are moved sequential in all three directions. After each measurement the support is moved back to the initial position. The movement is 20 mm in each direction.

The FEM-Model and the scans are modelled as NURBS. The comparisons between the initial position and the different movements show results like expected through the comparison of the FEM-Models in the same position. More interesting is the comparison between the FEM-Model and the scans in each position, because the scans show the actual measured state and the simulation the model state. For this comparison the scans are transformed with a classical 3D-Helmert-Transformation to the coordinate system of the FEM-Model. The transformation parameters are determined once in the initial position and used for all other positions, too. Multiple statistical tests are made for all positions. Due to this test there are no significant deviations, but the results are not realistic, because there are deviations bigger than 33 mm. One reason for the non-significant deviations could be correlations between the measurements. The next steps should be the integration of influences due to weather, waterproofing and grinding into the FEM-Model. For further scans the scanner errors should be investigated in detail and considered in the tests.

3.9. Location Referencing

With the growing availability of powerful and cost-efficient mobile devices as well as area-wide mobile communication networks, more and more applications are being developed in the consumer and professional sector (e.g. the automotive industry) that assign a location, the so-called georeference, to the transmitted information. In a geodetic sense, a georeference consists of a set of coordinates in a defined coordinate system and marks a place on earth in a distinct way. For practical application, however, it is often helpful to add links to real-world objects, e.g. buildings or roads to these coordinates. A catalogue of such mappings of real-world objects together with their description in general can be regarded as a (digital) map. To be able to exchange information that is referenced on objects of such a map, a standardized generalization of the georeference is required. This is typically referred to as Location Referencing.

Location Referencing techniques have been developed, implemented and practically utilized within a number of research projects. Within the EU-funded research project ROSATTE, for example, it became apparent that these LR-techniques are suitable for the transmission of map-based information between different map systems. For certain applications with high quality requirements, however, further improvements of these existing LR-methods are required.

Location Referencing can basically be differentiated in static and dynamic Location Referencing. Typical LR applications show a high dynamic together with high requirements on up-to-dateness and the need of immediate adaption to real-world changes. For that reason, a static referencing with centrally administrated location tables seems to be less reasonable for current and future practical applications of Location Referencing. Since it is already widely used and accessible with respect to its license and implementation, OpenLR is used and analysed in detail as a basis for further developments. For that reason, the corresponding OpenLR Whitepaper as the published standard and the reference implementation that is publicly available from the OpenLR website are investigated in detail and possibilities of improvement identified.

Based on the preceding analysis, a new Location Referencing method, the so-called form-matcher, has been developed in a thesis. The new method builds up on OpenLR, but uses additional, form-based matching parameters, e.g. the number of significant direction changes of a linear location reference. For the search for possible matching candidates, the complete course of the route of the location reference is considered in the target network. Then these identified route candidates are individually investigated using the selected matching parame-

ters. Furthermore, the new method considers the topological properties of the location references in particular for the decoding in the target network.

The quality specification of the map assignments and therewith also the evaluation of the LR transmissions should be based on existing quality models. Therefore, general approaches of quality specification of geodata in geoinformatics as well as the traffic and transportation domain, respectively, are investigated. Beyond that, existing approaches of quality description and modelling, for example the one derived from the ROSATTE research-project or the widely-used precision-recall approach are examined with respect to their suitability for the use.

Finally, the newly developed LR method together with the quality assessment methodology was implemented in the so-called LR testbed, to enable practical investigations. The empirical investigations that have been carried out using different datasets show a quality improvement of the form-matcher LR transmissions. For one direction (from map 1 one to map 2) of transmission, the share of correct assignments could be raised from 63 % to 75 %. For the opposite direction, however, OpenLR shows a higher quality level with a portion of 71 % of correct assignments that could not be improved by the form-matcher with its 69 % correctness.

3.10. Ghosthunter - Telematics System against ghost drivers using GNSS

In cooperation with the University of the Armed Forces Munich (UniBwM) and the company NavCert in Braunschweig, a telematics system will be implemented to detect ghost drivers with the use of GNSS and digital road maps, which could help to improve highway and auto safety greatly. A ghost driver is an individual who travels in a wrong direction or completely against the flow of traffic. Such wrong-way driving is responsible for about 2,000 accidents and 20 fatalities on the German autobahn every year, which are usually due to drunken driving or maybe also a suicide attempt. The purpose of the project called "Ghosthunter" is to contribute to preventing and managing ghost driver incidents.
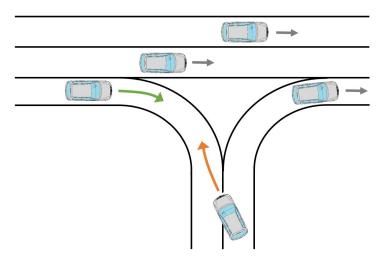

Figure 17: Ghost driver on German autobahn (source: UniBwM)

How can we detect ghost driving at an early stage and reliably, shake the wrong-way driver up efficiently and warn endangered road users in the surrounding area? In the project "Ghosthunter" this problem will be solved with a selected research method based on GNSS and spatial road maps. With a robust (D)GNSS-based algorithm developed by UniBwM, accurate vehicle trajectories (movement path) will be recorded and used in the map-matching algorithm to locate the vehicle on the road. However, before developing practical map-matching algorithms, data qualities of digital road maps of four different map providers (ATKIS, Here, TomTom and OSM) should be investigated with certain quality criteria. The absolute accuracy is evaluated by comparing every reference point (based on precise GNSS differential carrier-phase positioning) with its foot of perpendicular in the map line.

$$dx_i = x_{\text{gps},i} - x_{\text{lfp},i} \qquad (5)$$

$$dy_i = y_{\text{gps},i} - y_{\text{lfp},i} \qquad (6)$$

$$d_{x,y} = \sqrt{\Sigma_{i=1}^n \, dx_i^2 + dy_i^2} \qquad (7)$$

For valuating relative accuracy, two criteria will be chosen: one criterion is the difference of orientation changes between every map point and its homologous point of reference data

$$\Delta\Delta\alpha = \Delta\alpha_{\text{gps}} - \Delta\alpha_{\text{map}} \qquad (8)$$

and the other is the determination of the curvature difference between every map point and its homologous point of reference data.

$$\Delta\kappa = \kappa_{\text{gps}} - \kappa_{\text{map}} \qquad (9)$$

After reliable and comprehensive evaluations as well as consistency checks of ATKIS, Here, TomTom and OSM, the results show that all these four maps have reached an accuracy level of 2 meters for absolute position and 1 meter for relative accuracy.

4. Publications

Refereed Publications

Abdallah, A., Schwieger, V.: Kinematic Precise Point Positioning (PPP) Solution for Hydrographic Applications. FIG Working Week 2015, Sofia, Bulgaria, 2015.

Laufer, R., Schwieger, V.: Modeling Data Quality Using Artificial Neural Networks. In: Kutterer, H., Seitz, F., Alkhatib, H., Schmidt, M.: The 1st International Workshop on the Quality of Geodetic Observation and Monitoring Systems. Heidelberg, Springer, 2015.

Lerke, O., Schwieger V.: Evaluierung der Regelgüte für tachymetrisch gesteuerte Fahrzeuge. In zfv – Zeitschrift für Geodäsie, Geoinformation und Landmanagement, Heft 4/2015 – 140. Jahrgang.

Schmitt, A., Schwieger, V.: Quality Control of Robotics Made Timber Plates. FIG Working Week 2015, Sofia, Bulgaria, 2015.

Schweitzer, J., Schwieger, V.: Modeling and Propagation of Quality Parameters in Engineering Geodesy Processes in Civil Engineering. In: Kutterer, H., Seitz, F., Alkhatib, H., Schmidt, M.: The 1st International Workshop on the Quality of Geodetic Observation and Monitoring Systems. Heidelberg, Springer, 2015.

Non-Refereed Publications

Abdallah, A.: The Effect of Convergence Time on the Static-PPP Solution. Proceedings on 2nd International workshop on "Integration of Point- and Area-wise Geodetic Monitoring for Structures and Natural Objects", March 23-24, 2015, Stuttgart, Germany.

Abdallah, A., Schwieger, V.: PPP for Hydrography. GPS World Magazine, 26 (12), pp 52-55.

Al-Mistarehi, B., Schwieger, V.: Automated Detection for Pavement Crack for Mobile Mapping Data. Proceedings on 2nd International workshop on "Integration of Point- and Area-wise Geodetic Monitoring for Structures and Natural Objects", March 23-24, 2015, Stuttgart, Germany.

Breitenfeld, M.; Wirth, H.; Brüggemann, T.; Scheider, A.; Schwieger, V. (2015): Entwicklung von Echtzeit- und Postprocessingverfahren zur Verbesserung der bisherigen Ortung mit Glo-

bal Navigation Satellite Systems (GNSS) durch Kombination mit weiteren Sensoren sowie hydrologischen Daten. (Projektabschlussbericht HydrOs).

Karpik, A., Schwieger, V., Novitskaya, A., Lerke, O. (Hrsg.): Proceedings on 2nd International workshop on "Integration of Point- and Area-wise Geodetic Monitoring for Structures and Natural Objects", March 23-24, 2015, Stuttgart, Germany.

Kauker,S., Schwieger, V.: Approach for a Synthetic Covariance Matrix for Terrestrial Laser Scanner. Proceedings on 2nd International workshop on "Integration of Point- and Area-wise Geodetic Monitoring for Structures and Natural Objects", March 23-24, 2015, Stuttgart, Germany.

Schmitt, A.: Deformation Analysis of a Timber Pavilion. Proceedings on 2nd International workshop on "Integration of Point- and Area-wise Geodetic Monitoring for Structures and Natural Objects", March 23-24, 2015, Stuttgart, Germany.

Schwieger, V., Beetz, A.: Baumaschinensteuerung aus ingenieurgeodätischer Sicht. 145. DVW-Seminar: Interdisziplinäre Messaufgaben im Bauwesen - Darmstadt 2015, 26.-27.03.2015.

Schwieger, V., Schmitt, A.: Quality Control and Deformation Analysis for a Timber Construction. GeoSiberia 2015, Novosibirsk, Russia, 20.-22.04.2015.

Wirth, H., Breitenfeld, M., Scheider, A., Schwieger, V.: HydrOs - Ein integriertes Ortungssystem kombiniert mit hydrologischen Daten. Hydrographiosche Nachtrichten, Heft 6, 2015.

Zhang, L.: Reducing Multipath Effects by Considering Spatial Correlation. Proceedings on 2nd International workshop on "Integration of Point- and Area-wise Geodetic Monitoring for Structures and Natural Objects", March 23-24, 2015, Stuttgart, Germany.

Zhang, Lif., Zheng, B.: Denoising of the Point Cloud for Deformation Analysis. Proceedings on 2nd International workshop on "Integration of Point- and Area-wise Geodetic Monitoring for Structures and Natural Objects", March 23-24, 2015, Stuttgart, Germany.

Zhang, W., Zhang, L.: Time Series Analysis of Different Shieldings of Low-Cost GPS Receiver. Proceedings on 2nd International workshop on "Integration of Point- and Area-wise Geodetic Monitoring for Structures and Natural Objects", March 23-24, 2015, Stuttgart, Germany.

5. Presentations

Scheider, A.: „Erweiterung eines Multi-Sensorsystems zur Positionsbestimmung von Vermessungsschiffen", PhD-Seminar, DGK Section Engineering Geodesy, 7./8. May 2015, Stuttgart.

6. Activities at University and in National and International Organisations

Volker Schwieger
- Vice Dean of Faculty of Aerospace Engineering and Geodesy, University of Stuttgart
- Spokesperson of Centre for Transportation Research at University of Stuttgart (FOVUS)
- Executive Board of Cooperation German Rail (DB) and University of Stuttgart
- Chair of FIG Commission 5 "Positioning and Measurement"
- Head of Working Group III „Measurement Methods and Systems" of Deutscher Verein für Vermessungswesen (DVW)
- Chief Editor of Peer Review Process for FIG Working Weeks
- Member of Editorial Board Journal of Applied Geodesy

- Member of Editorial Board Journal of Applied Engineering Science
- Member of Editorial Board Journal of Geodesy and Geoinformation

Martin Metzner
- Member of the NA 005-03-01 AA "Geodäsie" at the DIN German Institute for Standardization

Li Zhang
- Vicechair of Administration of FIG Commission 5 "Positioning and Measurement"
- Member of Working Group III „Measurement Methods and Systems" of Deutscher Verein für Vermessungswesen (DVW)

7. Diploma Theses and Master Theses

Bosch, Jascha: Evaluierung der Regelgüte beim Einsatz von GNSS Sensoren im Baumaschinensimulator (Supervisor: O. Lerke)

Fedan, Mehdi: Design and development of a laser-scanning system for documentation of objects of cultural heritage (Supervisor: M. Metzner)

Haji Sheikhi, Meysam: Accuracy Analysis for the Low-Cost GPS Antennas with different Shieldings (Supervisor: L. Zhang)

Huang, Xingyun: Check the stability and independence of buildings movement for the measurement pillars in the measuring cellar (Supervisor: A. Hassan)

Kizilirmak, Gökhan: Detection and Reconstruction of the Catenary of a Rail Track Using Laser Scanning (Supervisor: M. Metzner)

Laatsch, Stephan: Vernetzung zweier Tachymeter zur automatischen Zielverfolgung (Supervisors: A. Scheider, O. Lerke)

Lafte, Meisam Alhajaj: Sensitivity Analysis and Design of Monitoring Networks Purposing Prediction of Landslides (Supervisor: O. Lerke)

Nanic, Milos: Development of the Vehicle and Motion Model for Construction Machines for a Kalman Filter (Supervisor: O. Lerke)

Obaid, Jehad: Map-Matching Algorithm: State of the Art and New Developments Concerning Real-Time Procedures and Open Street Map (Supervisor: M. Metzner)

Pitzer, Philipp: Ansatz zur Kartierung von Autobahnen für das autonome Fahren durch Mehrfachbefahrungen mittels potentieller Sensorik zukünftiger Serienfahrzeuge (Supervisor: M. Metzner)

Poptean, Sabina: Applications of terrestrial laser scanning and laser tracker for deformation analyses of a supporting structure (Supervisor: A. Schmitt)

Reuter, Philipp: Entwicklung eines Fuzzy-Reglers zur hochgenauen, autonomen Steuerung eines Baumaschinensimulators (Supervisor: O. Lerke)

Scatturin, Raphael: Entwicklung eines Kalman Filters für die Fusion von GPS- und Beschleunigungsdaten (Supervisors: A. Scheider, M. Metzner)

Schaal, Carolin: Deformationsuntersuchung am Rutschhang Hessigheim (Supervisor: A. Hassan)

Taschke, Simon: Contributions to the GNSS Positioning using virtual RINEX observation files. (Supervisor: L. Zhang)

Wang, Yuqi: Optimization of the Transient Oscillation during the Control of a Vehicle on a Given Trajectory (Supervisor: O. Lerke)

Ye, Zican: Untersuchung von TMC Nachrichten zum Nutzen in ADAS sowie Optimierung eines TMC-Generators (Supervisor: M. Metzner)

8. Study Theses and Bachelor Theses

Aichinger, Julia: Grundlagen und Beispielrechnungen zu NURBS (Supervisor: A. Schmitt)

Föll, Andreas: Untersuchung der Reflexivität unterschiedlicher Materialien (Investigations on the reflectivity of different materials) (Supervisor: S. Kauker)

Fischer, Jonas: Untersuchungen zur Kalibrierung des Laserstrackers API Radian. (Supervisor: A. Schmitt)

Graner, Martin: Echtzeit-Positionsbestimmung mittels bewegter Tachymeter (Supervisor: A. Scheider)

Kappeler, Marius: Evaluierung eines Tachymeters als bewegter Sensor in einem Positionierungssystem (Supervisor: A. Scheider)

Reuter, Philipp: Weiterentwicklung des Mobilen Positionierungssystems MOPSY (Supervisor: O. Lerke, M. Metzner)

Wenzl, Florian: Rekonstruktion der Portaloberfläche vom Münster zum Heiligen Kreuz für die Deformationsanalyse (Supervisor: B. Zheng, V. Schwieger)

9. Education

SS15 and WS15/16 with Lecture/Exercise/Practical Work/Seminar

Bachelor Geodesy and Geoinformatics:

Basic Geodetic Field Work (Schmitt, Kanzler) 0/0/5 days/0

Engineering Geodesy in Construction Processes (Schwieger, Kauker) 3/1/0/0

Geodetic Measurement Techniques I (Metzner, Schmitt) 3/1/0/0

Geodetic Measurement Techniques II (Schmitt) 0/1/0/0

Integrated Field Work (Metzner, Kauker) 0/0/10 days/0

Reorganisation of Rural Regions (Helfert) 1/0/0/0

Statistics and Error Theory (Schwieger, Zhang, Wang) 2/2/0/0

Master Geodesy and Geoinformatics:

Deformations Analysis (Schwieger, Zhang) 1/1/0/0

Industrial Metrology (Schwieger, Kanzler, Schmitt) 1/1/0/0

Land Development (Eisenmann) 1/0/0/0

Monitoring Project (Lerke) (0/0/2/0)

Monitoring Measurements (Schwieger, Wang) 1/1/0/0

Causes of Construction Deformation (Metzner/Scheider/Wang) 1/1/0/0

Transport Telematics (German) (Metzner, Scheider) 2/2/0/0

Thematic Cartography (German) (Metzner) 1/1/0/0

Terrestrial Multisensor Data Acquisition (German) (Zheng, Lerke) 1/1/0/0

Master GeoEngine:

Integrated Field Work (Metzner, Kauker) 0/0/10 days/0

Kinematic Measurement Systems (Schwieger, Lerke) 2/2/0/0

Monitoring (Schwieger, Wang) 1/1/0/0

Thematic Cartography (Metzner, Kauker) 1/1/0/0

Transport Telematics (Metzner, Hassan) 2/1/0/0

Bachelor and Master Aerospace Engineering:

Statistics for Aerospace Engineers (Schwieger, Zhang, Hassan) 1/1/0/0

Master Aerospace Engineering:

Transport Telematics (German) (Metzner, Scheider) 2/2/0/0

Bachelor Civil Engineering:

Geodesy in Civil Engineering (Metzner, Scheider) 2/2/0/0

Master Civil Engineering:

Geoinformation Systems (Metzner, Hassan) 2/1/0/0

Transport Telematics (Metzner, Scheider) 1/1/0/0

Bachelor Technique and Economy of Real Estate:

Acquisition and Management of Planning Data and Statistic (Metzner, Kanzler) 2/2/0/0

Bachelor Transport Engineering:

Statistics (Metzner, Kanzler) 0.5/0.5/0/0

Seminar Introduction in Transport Engineering (Hassan) 0/0/0/1

Master "Infrastructure Planning".

GIS-based Data Acquisition (Zhang, Schmitt) 1/1/0/0